6906–6918 *Nucleic Acids Research, 2020, Vol. 48, No. 12* *Published online 27 May 2020*
doi: 10.1093/nar/gkaa411

The hyperthermophilic partners *Nanoarchaeum* and *Ignicoccus* stabilize their tRNA T-loops via different but structurally equivalent modifications

Simon Rose[1], Sylvie Auxilien[2], Jesper F. Havelund[1], Finn Kirpekar[1], Harald Huber[3], Henri Grosjean[2] and Stephen Douthwaite[1,*]

[1]Department of Biochemistry & Molecular Biology, University of Southern Denmark, Campusvej 55, DK-5230 Odense M, Denmark, [2]Université Paris-Saclay, CEA, CNRS, Institute for Integrative Biology of the Cell (I2BC), 91198, Gif-sur-Yvette, France and [3]Lehrstuhl für Mikrobiologie und Archaeenzentrum, Universität Regensburg, Universitätsstraße 31, D-93053 Regensburg, Germany

Received February 08, 2020; Revised April 19, 2020; Editorial Decision May 04, 2020; Accepted May 06, 2020

ABSTRACT

The universal L-shaped tertiary structure of tRNAs is maintained with the help of nucleotide modifications within the D- and T-loops, and these modifications are most extensive within hyperthermophilic species. The obligate-commensal *Nanoarchaeum equitans* and its phylogenetically-distinct host *Ignicoccus hospitalis* grow physically coupled under identical hyperthermic conditions. We report here two fundamentally different routes by which these archaea modify the key conserved nucleotide U54 within their tRNA T-loops. In *N. equitans,* this nucleotide is methylated by the *S*-adenosylmethionine-dependent enzyme NEQ053 to form m^5U54, and a recombinant version of this enzyme maintains specificity for U54 in *Escherichia coli*. In *N. equitans*, m^5U54 is subsequently thiolated to form m^5s^2U54. In contrast, *I. hospitalis* isomerizes U54 to pseudouridine prior to methylating its *N1*-position and thiolating the *O4*-position of the nucleobase to form the previously uncharacterized nucleotide $m^1s^4\Psi$. The methyl and thiol groups in $m^1s^4\Psi$ and m^5s^2U are presented within the T-loop in a spatially identical manner that stabilizes the 3´-endo-*anti* conformation of nucleotide-54, facilitating stacking onto adjacent nucleotides and reverse-Hoogsteen pairing with nucleotide m^1A58. Thus, two distinct structurally-equivalent solutions have evolved independently and convergently to maintain the tertiary fold of tRNAs under extreme hyperthermic conditions.

INTRODUCTION

Stable tRNA and rRNA molecules function effectively to translate the genetic code into proteins only after a variety of posttranscriptional modifications have been added to their structures (1–5). Some RNA modifications are specific to certain groups of organisms, whereas others are highly conserved throughout the three domains of life. One such conserved modification is the 5-methyluridine at position 54 (m^5U54) in the T-loop of tRNAs. This nucleotide is universally conserved and is methylated in most members of the Bacteria and Eukarya (2,3) with only a few exceptions that include some members of the Mycoplasmatales (6–8). In archaeal tRNAs, m^5U54 has only been observed in the Thermococcales group (9), where it is typically modified further by thiolation to form m^5s^2U (10,11), as is also seen in some thermophilic bacteria (12–15). Uridine-54 is one of several nucleotides that are modified to facilitate the folding and stabilization of the core L-shaped conformation of tRNA (16,17). The density of such modifications is generally highest in thermophilic organisms that must maintain the structural integrity of their tRNAs under demanding environmental conditions (16,18,19).

In most organisms, the m^5U54 modification is catalyzed by an enzyme belonging to COG2265 (20), a family of pyrimidine methyltransferases that use *S*-adenosyl-L-methionine (AdoMet) as the methyl group donor. These m^5U54 methyltransferases are present in all three domains of life (21), and are exemplified by the bacterial homolog TrmA of *Escherichia coli* (22–24), the eukaryotic enzyme Trm2p seen in *Saccharomyces cerevisiae* (25), and the euryarchaeota homolog PAB0719 (TrmU54) from *Pyrococcus abyssi* (9,26). The importance of U54 methylation is underlined by the existence of an alternative and phylogenetically-unrelated mechanism directed by the COG1206 flavoprotein TrmFO (27–30), which catalyzes

*To whom correspondence should be addressed. Tel: +45 6550 2395; Email: srd@bmb.sdu.dk

m^5U54 formation using N^5,N^{10}-methylenetetrahydrofolate as the methyl group donor (31).

In hyperthermophilic organisms where m^5U54 is modified further to form m^5s^2U, the bulky sulphur atom constrains the ribose pucker in the 3′-endo configuration to avoid a steric clash with the 2′-hydroxyl (32) favouring the *anti*-orientation of the U54 base. This in turn promotes U54 stacking onto adjacent nucleotides and its reverse-Hoogsteen pairing with A58 within the T-loop (33), the net effect of which is to increase the thermostability of the tRNA (14,32,34,35). However, nucleotide m^5s^2U is absent in the tRNAs of hyperthermophilic archaea of the Crenarchaeota phylum (10), and these organisms modified uridine-54 via an alternative route to form $m^1\Psi$ (36). Nucleotide $m^1\Psi54$ engages in similar interactions within the T-loop, including a reverse-Hoogsteen pairing with A58 (37). The extent to which the different U54 modifications in Crenarchaeota and the Thermococcales branch of the Euryarchaeota are physiologically equivalent has not been previously known, and this question is addressed in the present study.

The hyperthermophilic archaea *Ignicoccus hospitalis* and *Nanoarchaeum equitans* grow physically attached as a commensal pair under identical environmental conditions (38). *I. hospitalis* is a member of the Crenarchaeota, whereas *N. equitans* is closer to the Euryarchaeota (39,40) and has more recently been placed in the Nanoarchaeota branch of the DPANN superphylum (41). *I. hospitalis* has a genome encoding almost 1500 open reading frames (ORFs) (42) and grows perfectly well as a pure culture, whereas *N. equitans* has a considerably smaller genome of 552 ORFs (43), and proliferates only when physically attached to its *I. hospitalis* host (38,39). The genomes of these two archaea encode different complements of RNA modification enzymes. Here we use liquid chromatography with mass spectrometry to map the modifications at and around nucleotide U54 to determine how the two archaea stabilize their tRNA tertiary structures. We show that despite the coupled growth of *N. equitans* and *I. hospitalis* under identical hyperthermic conditions, the two archaea modify their tRNAs in distinctly different ways. While *N. equitans* modifies U54 to form m^5s^2U, *I. hospitalis* synthesizes the previously uncharacterized nucleotide $m^1s^4\Psi54$, which stabilizes the tRNA T-loop in a structurally equivalent manner.

MATERIALS AND METHODS

In silico screening of the *I. hospitalis* and *N. equitans* genomes

Previously characterized m^5U RNA methyltransferases were used as BLAST queries (44) against open reading frames (ORFs) in *I. hospitalis* and *N. equitans*. These included the AdoMet-dependent RlmD (UniProt accession number P55135) and TrmA (P23003) methyltransferases from *E. coli* K12, the *P. abyssi* methyltransferases PAB0719 (Q9UZR7) and PAB0760 (Q9UZK1), and the folate-dependent enzymes TrmFO (P39815) from *Bacillus subtilis,* and RlmFO (Q2SS13) from *Mycoplasma capricolum* (45).

The *I. hospitalis* and *N. equitans* genomes were also screened for homologs of TtuA and TtuB that direct thiolation of m^5U54 (46), and the Pus10/TrmY combination that produces $m^1\Psi54$ (47). BLAST queries included the *P. abyssi* and *Pyrococcus furiosus* homologs PAB1092 and PF0273 (TtuA), PF1758 (TtuB), PAB2391 and PF1139 (Pus10) and PAB1866 (TrmY).

Growth of *I. hospitalis*/*N. equitans*

I. hospitalis was grown on its own in pure culture and in co-culture with *N. equitans* as previously described (39). Cells were harvested at late log phase by centrifugation, and *N. equitans* cells were enriched from the co-cultures by differential centrifugation (39). Cells were run twice through a French press, followed by addition of 4 ml of TRIzol® (Life Technologies). After 5 min at 20°C, 0.8 ml chloroform was added, and the samples were centrifuged at 12,000 g for 5 min. The aqueous phase was extracted with phenol/chloroform, before collecting the nucleic acids by ethanol precipitation.

Analyses of tRNAs nucleosides

The total RNA mixtures from *I. hospitalis* (pure culture) or *N. equitans* (enriched from co-cultures) were extracted with Nucleobond® RNA/DNA 400 kits (Macherey-Nagel) to isolate the tRNA fractions. The supernatant fractions containing tRNAs and other soluble RNAs were passed through Microcon YM-100 columns (Millipore) to reduce the amount of impurities. The supernatant samples were digested to completion to form nucleosides (48) and analyzed using an Agilent Technologies 1100 HPLC with a Hypercarb column (150 mm × 0.3 mm) containing 5 μm PGC pore size of 250 Å (Thermo Scientific) and run at 0.5 μl/min. Nucleosides were separated using gradients of 0–90% acetonitrile in 0.1% formic acid and were detected by absorbance at 260 nm.

Nucleoside structures were subsequently determined by liquid chromatography (LC) linked with electrospray ionization (ESI) quadrupole time of flight mass spectrometry (qToF-MS) using Agilent 6530B equipment. Total tRNA nucleosides, prepared as above, were lyophilized, resuspended in 15 μl 0.1% formic acid and centrifuged at 16,000 g for 5 min. The supernatant, in 4 μl portions, was injected into an Agilent Technologies 1290 Infinity HPLC system equipped with an Agilent Zorbax Eclipse Plus C18 column (2.1 × 150 mm, 1.8 μm) and a 50 mm guard-column at 40°C. A chromatographic gradient was formed from 0.1% formic acid in water (solvent A) and 0.1% formic acid in acetonitrile (solvent B) by increasing the proportion of solvent B from 3 to 95% over 10 min at a flow rate of 400 μl/min. Elutants were analyzed by qToF-MS scanning three time per second from m/z 50 to m/z 1050 at a gas temperature of 325°C with drying gas at 8 l/min, nebulizer at 35 psig, sheath gas temp 350°C, sheath gas flow at 11 min/l, V_{Cap} at 3500 V, fragmentor at 125 V and skimmer at 65 V. Spectra were calibrated from the signals of purine and Hexakis (1H,1H,3H-tetrafluoropropoxy) phosphazine delivered through a second needle in the ion source by an isocratic

pump (flow rate 20 μl/min). Nucleosides were compared to chemically synthesized standards (Um, m^5U, s^2U, s^4U, m^5s^2U, Ψ, $s^2Ψ$, $m^1Ψ$, $m^3Ψ$ and $m^1m^3Ψ$). Tandem MS fragmentation (MS/MS) was carried out in positive and negative ion modes at collision energies of 35 V and 15V, respectively. In order to promote fragmentation of s^2U and s^4U for comparison to compound #8, the fragmentor voltage was increased to 190V before selecting the protonated nucleobases for MS/MS (pseudo-MS^3). Ion chromatograms were extracted using 5 ppm mass tolerance, and spectra were analyzed using Masshunter Qualitative Analysis B.08.00 (Agilent). Oligonucleotide masses and isotope distribution were calculated using the software at https://www.envipat.eawag.ch/.

In the experiments where recombinant NEQ053 was expressed in *E. coli*, tRNA nucleoside masses and fragmentation patterns were determined after LC separation by a different analytical set-up using ion-trap ESI-MS, as previously reported (48).

Expression and purification of recombinant NEQ053

The NEQ053 open reading frame was amplified by PCR using *N. equitans* chromosomal DNA as template. This region of the *N. equitans* chromosome encodes an ATG sequence 27 codons upstream and in-frame with a second ATG and, by alignment with pyrococcal and other homologs, we judged the second ATG to be the true start of the NEQ053 ORF. Our PCR product, extending from this second ATG, was inserted into the *E. coli* expression vector pQE-80L (QIAGEN) to encode a protein with an *N*-terminal tag of six histidine residues. Purification of the NEQ053 enzyme to near homogeneity was achieved by chromatography on Ni-NTA resin (QIAGEN) and a HiTrap™ Heparin column (GE Healthcare) (9). Enzyme fractions were pooled and run over a PD10 column (GE Healthcare) equilibrated with 25 mM Tris-HCl pH 7.5, 300 mM NaCl, 10% glycerol and 2 mM DTT. The NEQ053 enzyme was stored in aliquots at –80°C. The methyltransferase function of the recombinant NEQ053 was also tested *in vivo* in *E. coli* after expressing from a plasmid (49) in an *rlmC, rlmD, trmA* null-strain lacking all endogenous m^5U RNA modifications (50).

In vitro transcription and methylation of *N. equitans* $tRNA^{Thr}$

A double-stranded DNA template for *N. equitans* $tRNA^{Thr}$ (anticodon GGU) was produced by PCR using the Vent DNA polymerase (New England Biolabs) and two oligodeoxynucleotides with overlapping ends where one of these primers contained the T7 promoter sequence (51). The $tRNA^{Thr}$ transcript was purified on a denaturing gel (52), and 500 nM was incubated with 20 nM of recombinant NEQ053 methyltransferase for 15 min at 80°C in 25 μl methylation buffer consisting of 25 mM Tris–Cl, pH 7.5, 50 mM ammonium acetate, 2 mM dithiotreitol, 10 mM $MgCl_2$, 0.1 mg/ml RNase-free bovine serum albumin (Roche Applied Science) and 80 μM AdoMet (Sigma). Reactions were stopped by extracting with phenol/chloroform and the tRNA was recovered by ethanol precipitation.

Analysis of rRNA and tRNA sequences by MALDI-ToF

In vitro methylation by NEQ053 in the *N. equitans* $tRNA^{Thr}$ was analyzed directly by MALDI-ToF after digestion with RNase A or T1. MALDI analyses of the much larger rRNAs required prior isolation of fragments of approximately 50 nucleotides using DNA oligonucleotides complementary to the *I. hospitalis* and *N. equitans* 23S rRNA sequences 720–770, 1890–1945 and 1910–1960. DNA oligos at 1 nmol were mixed in 62.5 mM HEPES, pH 7.0 and 125 mM KCl with 300 pmol of total RNA from pure cultures of *I. hospitalis* or *N. equitans* enriched from co-culture and were heated at 90°C for 5 min followed by slow cooling to 37°C. The same rRNA regions were isolated from the *E. coli rlmC, rlmD, trmA* null-strain recombinants (50,53). The oligonucleotide-rRNA hybrids were digested with RNase A and mung bean nuclease, and protected rRNA fragments of approximately the same length as the oligonucleotides were isolated on gels (54,55). RNase cleavage at any mismatched sites in the rRNA-oligonucleotide hybrids effectively separated any *I. hospitalis* rRNAs impurities in the *N. equitans* samples (49). Sites of modification in the rRNA fragments and in tRNA transcripts were identified by digesting with RNase A or T1 and analyzing the resultant oligonucleotides using MALDI-TOF mass spectrometry (UltrafleXtreme, Bruker Daltonics) collecting data in positive ion mode (54,55).

Primer extension

Primer extension was used to investigate sites of 2′-*O*-methylation in *N. equitans* 23S rRNA that had been indicated by MALDI-MS. 3 pmol Cy5-labelled DNA primers of 18–20 nucleotides were hybridized to complementary sequences within *N. equitans* 23S rRNA (4 pmol) by incubating at 80°C for 2 min in 4.5 μl of 56 mM HEPES pH 7.0 and 112 mM KCl followed by slow cooling to 42°C. Extension and sequencing reactions were performed with 1.5 U AMV reverse transcriptase (Thermo Scientific) per reaction (56) and analyzed on 13% polyacrylamide-urea gels. Bands were visualized on a Typhoon FLA 9500 from GE Healthcare.

RESULTS

Screening for candidate m^5U methyltransferases

In silico analyses of the genome sequences showed that NEQ053 from *N. equitans* was the only ORF to score an *E*-value that is compatible with an RNA m^5U methyltransferase. In comparison with methyltransferase homologs for which the RNA targets have already been empirically characterized, the best score for NEQ053 was against *P. abyssi* PAB0719 (TrmU54) with an *E*-value of 10^{-101}, while the paralogous enzyme PAB0760, which is specific for U747 in 23S rRNA, gave an *E*-value of 10^{-80}. However, a different pattern was seen when compared with bacterial enzymes, where *E. coli* RlmD specific for U1939 in 23S rRNA was more similar to NEQ053 (E-value 10^{-35}) than its U54-specific counterpart TrmA (*E*-value 10^{-15}). No ORF with significant similarity to the folate-dependent m^5U methyltransferases RrmFO or TrmFO was

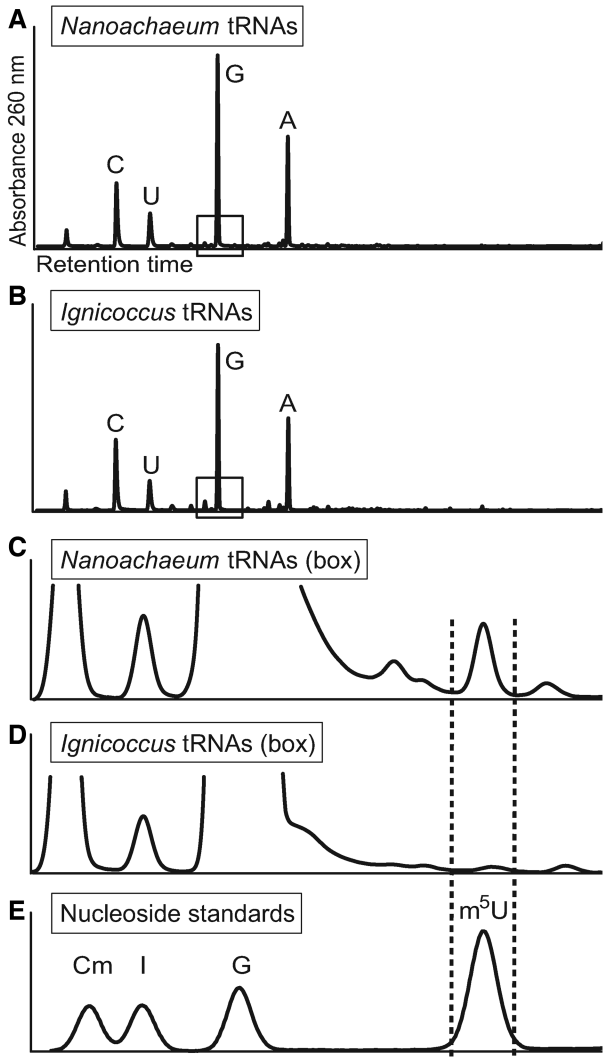

Figure 1. HPLC profiles of tRNA nucleosides from *Nanoarchaeum* and *Ignicoccus* cells. (**A**) Nucleosides from the enriched *Nanoarchaeum* culture, and (**B**) from *Ignicoccus* cultured alone. (**C**) Enlargement of the boxed region in panel A containing m^5U, and (**D**) the same region from panel B showing the absence of m^5U. (**E**) Nucleoside standardization mixture, indicating the fraction corresponding to the retention time for m^5U.

detected. No gene encoding a homolog of any previously characterized RNA m^5U methyltransferase was found in the *I. hospitalis* genome.

Verification of tRNA m^5U by HPLC

The bioinformatics findings were tested by assaying for m^5U in the archaeal tRNAs. Nucleosides hydrolysates were generated from bulk tRNAs isolated from pure cultures of *I. hospitalis* and from co-cultures after enrichment of *N. equitans*, and were analyzed by HPLC (Figure 1). Consistent with the absence of an RNA m^5U methyltransferase, no m^5U was present in nucleosides isolated from pure cultures of *I. hospitalis* cells. In the *N. equitans* tRNA nucleosides, m^5U was present (Figure 1C) but constituted only about 3% of the total amount of uridine. Based on their average uridine content, this indicates that approximately one quarter of *N. equitans* tRNAs contained this single modification.

NEQ053 is responsible for tRNA m^5U54 modification

An *in vitro* system with a recombinant version of NEQ053 and an unmodified transcript of *N. equitans* $tRNA^{Thr}$ was used to establish whether this enzyme was responsible for adding m^5U and to identify the location of the modification in the tRNA structure. This tRNA substrate generates RNase digestion products that are easily distinguishable by MALDI-MS. After incubation with NEQ053 and digestion with RNase A, a spectral shift occurred in the unique fragment GGGUp containing nucleotide U54 due to a mass increase of 14.0 Da (Figure 2). This mass change is consistent with substitution of a hydrogen atom with a methyl group. The same increase in the overlapping RNase T1 fragment UUCGp established the exact location of the methylation at nucleotide U54 and confirmed that modification here was stoichiometric.

Expression of NEQ053 in *E. coli* and screening for additional m^5U targets

An *E. coli* strain in which *rlmC, rlmD* and *trmA* had been inactivated, and thus lacked m^5U modifications in its rRNAs and tRNAs, was used as a host for expressing the recombinant NEQ053. HPLC analysis of bulk tRNAs showed that NEQ053 added m^5U to the tRNAs within the *E. coli* null-strain (Supplementary Figure S1). Generation of a nucleoside with a mass corresponding to methylated uridine was confirmed by ESI-MS (Supplementary Figure S1), and its collision-induced fragmentation generated a pattern of masses that unambiguously matched an m^5U standard (Supplementary Figure S1C), confirming the site of methyl group addition on the *C5*-atom of the uracil base.

Isolation of the nucleotide regions around *E. coli* 23S rRNA U747 and U1939 and their analysis by MALDI-MS showed that there was no rescue of modification at these other nucleotide targets by NEQ053 (not shown). Similar analyses also ruled out the presence of m^5U modification at the equivalent locations in *N. equitans* 23S rRNA (Supplementary Figure S2). In the course of these studies, numerous sites of 2′-*O*-methylation within the *N. equitans* 23S rRNA structures around nucleotide 1939 were revealed by MS and verified by primer extension (Supplementary Figure S2).

In silico screening for supplementary enzymes modifying U54

The relatively low amount of m^5U in tRNAs extracted from *N. equitans* cells (Figure 1) was clearly inconsistent with the activity of this enzyme when tested *in vitro* (Figure 2) and *in vivo* in the heterologous *E. coli* host (Supplementary Figure S1). We reasoned that the low yield of m^5U in *N. equitans* cells could indicate that it represented a precursor that would subsequently be converted into a hypermodified form. *In silico* screening of the archaeal genomes for ORFs encoding additional uridine modification enzymes revealed homologs of TtuA and TtuB that thiolate the 2-position of m^5U in tRNAs. The *N. equitans* ORF NEQ283 showed high

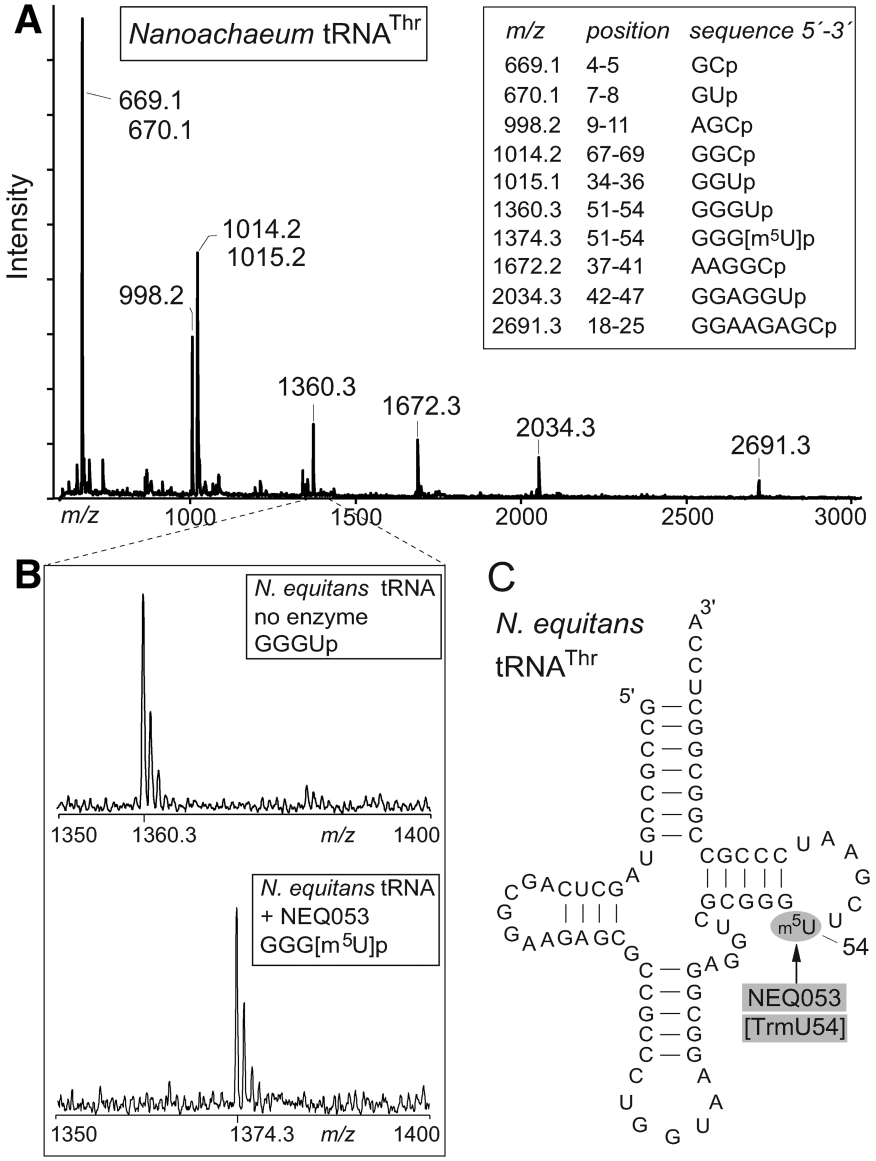

Figure 2. MALDI-MS spectra showing methylation *in vitro* by NEQ053 at U54 in *N. equitans* $tRNA^{Thr}$. (**A**) Spectrum of oligonucleotides formed by RNase A digestion of unmodified $tRNA^{Thr}$. The measured mass/charge (m/z) of each fragment is shown above the peak with the theoretical m/z values (in box). (**B**) Enlargement of the spectral region containing the GGGUp fragment from nucleotides 51–54 with an m/z of 1360.3 when derived from the unmodified $tRNA^{Thr}$, and with m/z of 1374.3 after incubation of the tRNA *in vitro* with NEQ053 prior to digestion. (**C**) Schematic of the *N. equitans* $tRNA^{Thr}$ secondary structure. The target site of NEQ053 indicates that the enzyme could be renamed as TrmU54.

similarity to PF0273, a TtuA homolog from *P. furiosus* (*E*-value = 10^{-53}), while NEQ523 displayed close resemblance to the TtuB homolog PF1758 (*E*-value = 10^{-73}).

A database search for enzymes that might modify U54 in *I. hospitalis* tRNAs revealed Igni_0342, a homolog of the pyrococcal enzyme Pus10 that isomerizes this nucleotide to Ψ (*E*-values of 10^{-77} against PAB2391 and PF1139). In a subsequent modification step seen in many archaeal species, the methyltransferase TrmY converts the pseudouridine to $m^1\Psi$. A likely candidate for catalyzing this reaction was the *I. hospitalis* protein Igni_0291, which shows an *E*-value of 10^{-27} against the *P. abyssi* TrmY homolog PAB1866. No homologs of Pus10 or TrmY were found in *N. equitans*.

Database searches also showed that the *I. hospitalis* genome encodes orthologs of the two putative U54 thiolation enzymes, TtuA and TtuB, where Igni_0707 resembles NEQ283 (*E*-value = 10^{-31}) and Igni_0506 is similar to NEQ523 (*E*-value = 10^{-42}). In the absence of the modification pathway through m^5U, this raised the possibility that these *I. hospitalis* enzymes might thiolate $m^1\Psi 54$ forming a previously unseen hypermodified version of this nucleotide.

Uridine hypermodification in the archaeal tRNAs

The putative functions of the enzymes predicted by the bioinformatics searches described above were tested by

fractionating nucleosides from the *N. equitans* and *I. hospitalis* tRNAs by liquid chromatography and defining their masses using ESI-MS. Nucleoside structures were determined from their collision-induced fragmentation and comparison of the fragment patterns with those of known uridine derivatives.

Eleven distinct derivatives of uridine were isolated from the two sets of archaeal tRNAs (Table 1). With a couple of notable exceptions, these matched the retention times, masses and fragmentation patterns of known standards, thus making identification straightforward and unequivocal. Unmodified uridine was the predominant component and eluted immediately after pseudouridine on the LC; both nucleotides (compounds #1 and #2, Table 1) have the same monoisotopic mass of 244.07 Da (m/z 245.08 in positive ion mode; monoisotopic masses are used throughout). Three nucleosides of mass 258.08 Da (m/z 259.09 in positive ion mode) were identified as uridines with a single methyl group. The first of these to elute, $m^1\Psi$ (compound #3), was in small amounts and specific to *I. hospitalis;* the next, m^5U (compound #4), was also in small amounts and specific to *N. equitans*; while the third nucleoside with this mass, Um (compound #5), gave a prominent peak for both organisms (Figure 3A and Supplementary Figure S3).

Three nucleosides were observed at m/z 275.07, which fits the mass of a methylated uridine with a thiol group (Figure 3B). One of these (compound #7, Table 1) was specific to *N. equitans* and was unambiguously identified as m^5s^2U by fragmentation and comparison to a chemically synthesized standard (Figure 3B).

The other two nucleosides (#6 and #8) originated in *I. hospitalis* and have the same mass as m^5s^2U (within the accuracy of the instrumentation used here), but with LC retention times that indicate distinctly different structures. Our spectrometric set-up has a mass accuracy better than 5 ppm and this, together with analysis of isotope patterns, is a strong predictor of atomic composition. The five top candidates that match the observed mass/isotope pattern of compound #6 are listed in Supplementary Table S1. From these, the atomic composition $C_{10}N_2O_5SH_{14}$ is the best candidate, and fits with the structure of a methylated and thiolated uridine/pseudouridine. The second-best candidate ($C_{11}N_6OSH_{10}$) is very close in score and also in its predicted isotope distribution (Supplementary Figure S4), however, this composition has only a single oxygen making it incompatible with a nucleoside. Apart from m^5s^2U, no standards with the composition $C_{10}N_2O_5SH_{14}$ are available for direct experimental comparison, and therefore the structure of compound #6 was deduced by piecing together distinguishing fragments (and ruling out others) from the set of uridine derivatives in Table 1.

First, it was established that compound #6 is a derivative of pseudouridine. The main positive-ion fragmentation pathway for all nucleosides, except pseudouridine and its derivates, is loss of the sugar moiety. Compound #6 has a stable glycosidic bond (Figure 4) and produces no fragments corresponding to loss of ribose- or methylated ribose-derivatives (theoretically, at m/z 129.01 and 143.03, respectively). Further, there is significant overlap with the $m^1\Psi$ fragmentation pattern, indicating that compound #6 is methylated on the *N1*-position. In addition, some of these fragments show distinctive mass shifts corresponding to the substitution of an oxygen atom with sulphur (Figure 4). Finally, the position of this thiol group at the 4-carbonyl rather than the 2-carbonyl position was deduced from similarities and differences to aspects of $s^2\Psi$ and $m^1\Psi$ negative ion-mode fragmentation (Figure 5). These fragmentation data, together with the atomic composition derived from the accurate mass and the isotope distribution (Table S1 and Supplementary Figure S4), indicate that compound #6 is $m^1s^4\Psi$.

The minor product compound #8 was identified through the same mass accuracy/isotope considerations used for compound #6, and additionally by comparison of its fragmentation pattern against s^2U, s^4U and Um standards (Supplementary Figure S5). The characteristic neutral loss of 146.06 Da, corresponding to a methylated ribose-derivative, and a base-fragmentation pattern identical to that of s^2U, allow us to conclude that compound #8 is s^2Um.

Three uridines with a single thiol and no methyl group (compounds #9, #10 and #11) were identified. Compounds #10 and #11 are present in both archaea and were identified as s^2U and s^4U, respectively, in a straightforward comparison with known standards (Supplementary Figure S5). Compound #9 was present only in *N. equitans,* and in low quantities. Here, no standard with the same mass and retention time was available. Fragment data indicate that the structure is most likely to be $s^4\Psi$ (Supplementary Figure S6), but with a lower degree of certainty than for the other nucleosides in Table 1.

Compound #12 was found only in *I. hospitalis* tRNAs (Table 1). The mass of this compound and the resilience of its glycosidic bond under fragmentation showed it to be dimethyl pseudouridine. Comparison with the $m^1m^3\Psi$ standard ruled out this structure, while similarity to $m^1\Psi$, with a 14 Da increase in the masses of fragments that include the 2′-ribose position, indicate that compound #12 is $m^1\Psi m$.

DISCUSSION

N. equitans grows physically attached to the surface of *I. hospitalis,* and the two archaea thus experience identical environmental conditions where temperatures can exceed 95°C. These organisms are, however, phylogenetically distinct with *I. hospitalis* belonging to the Crenarchaeota while *N. equitans* is closer to the Euryarchaeota (40) within the Nanoarchaeota phylum of the DPANN superphylum (41). Both organisms possess highly truncated genomes and while *I. hospitalis* is self-sufficient, *N. equitans* lacks many metabolic enzymes and compensates by scavenging small essential compounds from *I. hospitalis* over their fused cell membranes (38,39). It seems unlikely, however, that larger molecules such as RNA modification enzymes are transported between the two organisms (49), and raises the question of how their tRNA molecules are stabilized to enable them to survive and thrive together under the same extreme conditions.

The *N. equitans* enzyme NEQ053 was a clear candidate for an m^5U methyltransferase with an E-value of 10^{-101}

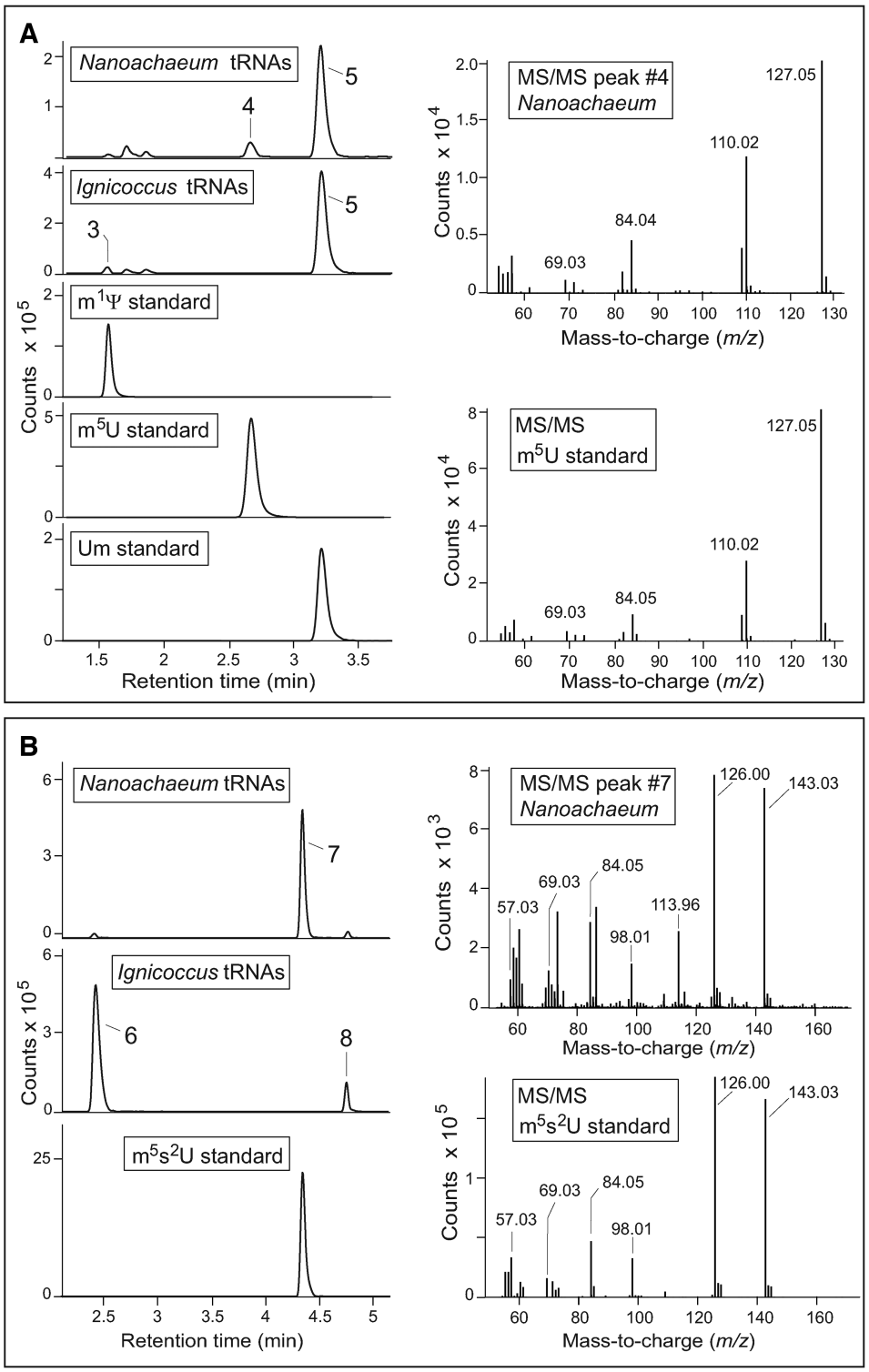

Figure 3. LC/ESI-MS characterization of uridine nucleosides from *N. equitans* and *I. hospitalis* tRNAs. (**A**) Analyses of uridines modified with one methyl group and registered at *m/z* 259.09 in positive ion mode. On left, retention times during liquid chromatography compared to known methyluridine standards. On right, fragmentation of *N. equitans* compound #4 confirming its structure from comparison with the m^5U standard. The identities of compound #3 ($m^1\Psi$) and compound #5 (Um) were verified by the same methods (Supplementary Figure S3). Minor amounts of non-nucleoside compounds can be seen migrating at retention times close to that of $m^1\Psi$. (**B**) Uridines modified with a methyl plus a thiol group registered at *m/z* 275.07 in positive ion mode. Compound #7 is specific to *N. equitans* and matches the LC profile of the m^5s^2U standard as well as its MS/MS fragmentation pattern (right). No standards with the same LC migration were available for compounds #6 and #8, and these were identified respectively as $m^1s^4\Psi$ and s^2Um by comparing their fragmentation patterns to a series of nucleosides containing these individual modifications (Figures 4 and 5). Small quantities of these compounds were observed in some preparations of the enriched *N. equitans* cells (as seen here) and are contaminants resulting from incomplete removal of all the *I. hospitalis* cells.

Table 1. Uridine nucleoside derivatives identified in the tRNAs of *N. equitans* and *I. hospitalis*

Compound notation and retention time (RT in min)		Archaeon	*m/z* (negative/positive ion modes)	Molecular composition	Nucleoside	Nucleoside standards for comparison	Notes
#1	1.2	*I. hospitalis & N. equitans*	243.062/245.077	$C_9H_{12}N_2O_6$	Ψ	Ψ	a
#2	1.5	*I. hospitalis & N. equitans*	243.062/245.077	$C_9H_{12}N_2O_6$	U	U	a
#3	1.5	*I. hospitalis*	257.078/259.093	$C_{10}H_{14}N_2O_6$	$m^1\Psi$	$m^1\Psi$	a,b
#4	2.6	*N. equitans*	257.078/259.093	$C_{10}H_{14}N_2O_6$	m^5U	m^5U	a,b
#5	3.2	*I. hospitalis & N. equitans*	257.078/259.093	$C_{10}H_{14}N_2O_6$	Um	Um	a
#6	2.5	*I. hospitalis*	273.055/275.070	$C_{10}H_{14}N_2O_5S$	$m^1s^4\Psi$	Ψ, $m^1\Psi$, $s^2\Psi$	c
#7	4.4	*N. equitans*	273.055/275.070	$C_{10}H_{14}N_2O_5S$	m^5s^2U	m^5s^2U	a
#8	4.8	*I. hospitalis*	273.055/275.070	$C_{10}H_{14}N_2O_5S$	s^2Um	m^5s^2U, s^2U, s^4U, Um	c
#9	1.6	*N. equitans*	259.039/261.054	$C_9H_{12}N_2O_5S$	$s^4\Psi$	Ψ, $s^2\Psi$	b,c
#10	3.0	*I. hospitalis & N. equitans*	259.039/261.054	$C_9H_{12}N_2O_5S$	s^2U	s^2U	a
#11	3.7	*I. hospitalis & N. equitans*	259.039/261.054	$C_9H_{12}N_2O_5S$	s^4U	s^4U	a
#12	3.0	*I. hospitalis*	271.094/273.108	$C_{11}H_{16}N_2O_6$	$m^1\Psi m$	$m^1\Psi$, $m^3\Psi$, m^1U	c

[a]Structures confirmed by mass determination, chromatographic retention time (RT) and tandem MS (MS/MS) fragmentation analyses of compound and comparison with identical chemically synthesized standard.
[b]Present in small amounts compared to the other modified nucleosides.
[c]No identical synthetic standard available. Structures deduced from mass determination, isotope distribution, tandem MS analyses and comparison with related (nonidentical) standards to identify and exclude known nucleoside fragments.

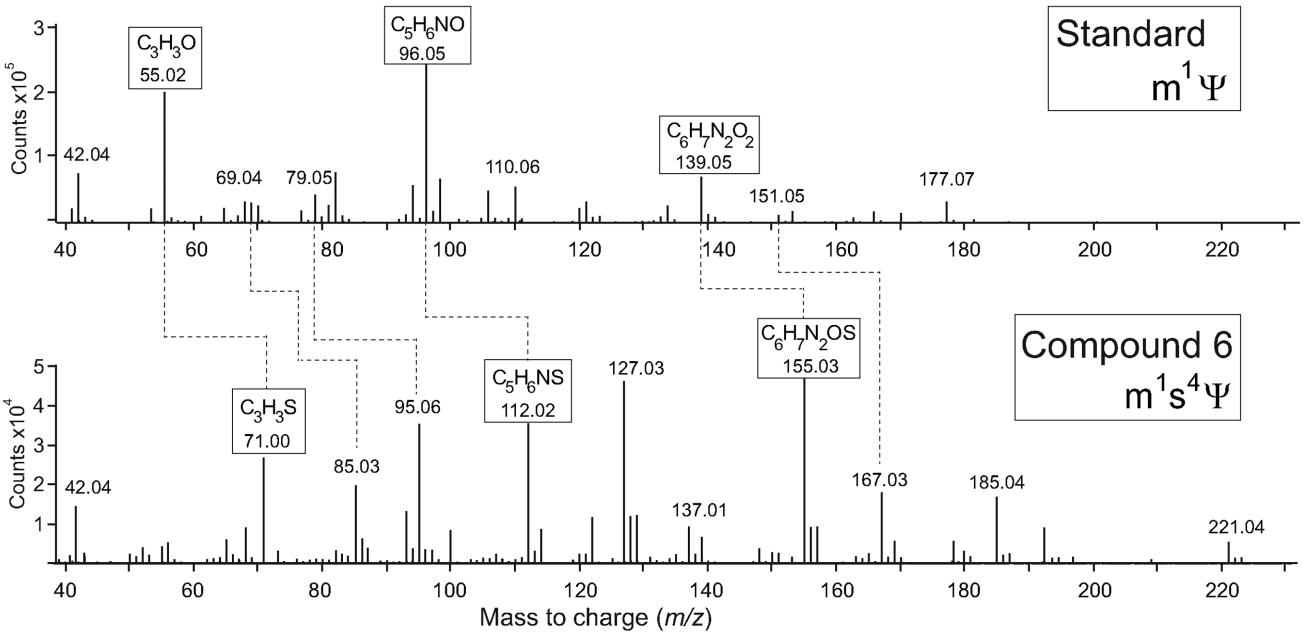

Figure 4. Tandem MS in positive ion mode of compound #6 comparing with the fragmentation pattern of $m^1\Psi$. Key fragments are indicated in boxes, and are seen to increase in mass by 16 Da showing *O*- to *S*- substitution. The fragmentation pattern is consistent with compound #6 being $m^1s^4\Psi$. The positions of the methyl group at *N1* and the sulphur on *C4* of the pseudouridine were conclusively verified by fragmentation in the negative ion mode and comparison with additional standards (Figure 5).

against PAB0719 that has previously been shown to add the m^5U54 modification in *P. abyssi* tRNAs (9). However, in addition to tRNA-specific methyltransferases, the COG2265 group also contains the closely related enzymes RlmC and RlmD, which respectively add m^5U modifications at U747 and U1939 in bacterial 23S rRNA (53,57). When compared with the bacterial enzymes, the NEQ053 sequence shows greater similarity to RlmD than its U54-specific counterpart TrmA, and is furthermore highly similar to the *P. abyssi* paralog PAB0760 that is responsible for m^5U747 modification in 23S rRNA (51). Such ambiguity in bioinformatics-based prediction of pyrimidine *C5*-methylation targets has already been noted in previous studies, where empirical testing was required to identify the nucleotide target (51,58) and in one case revealed dual RNA modification sites (50). We therefore

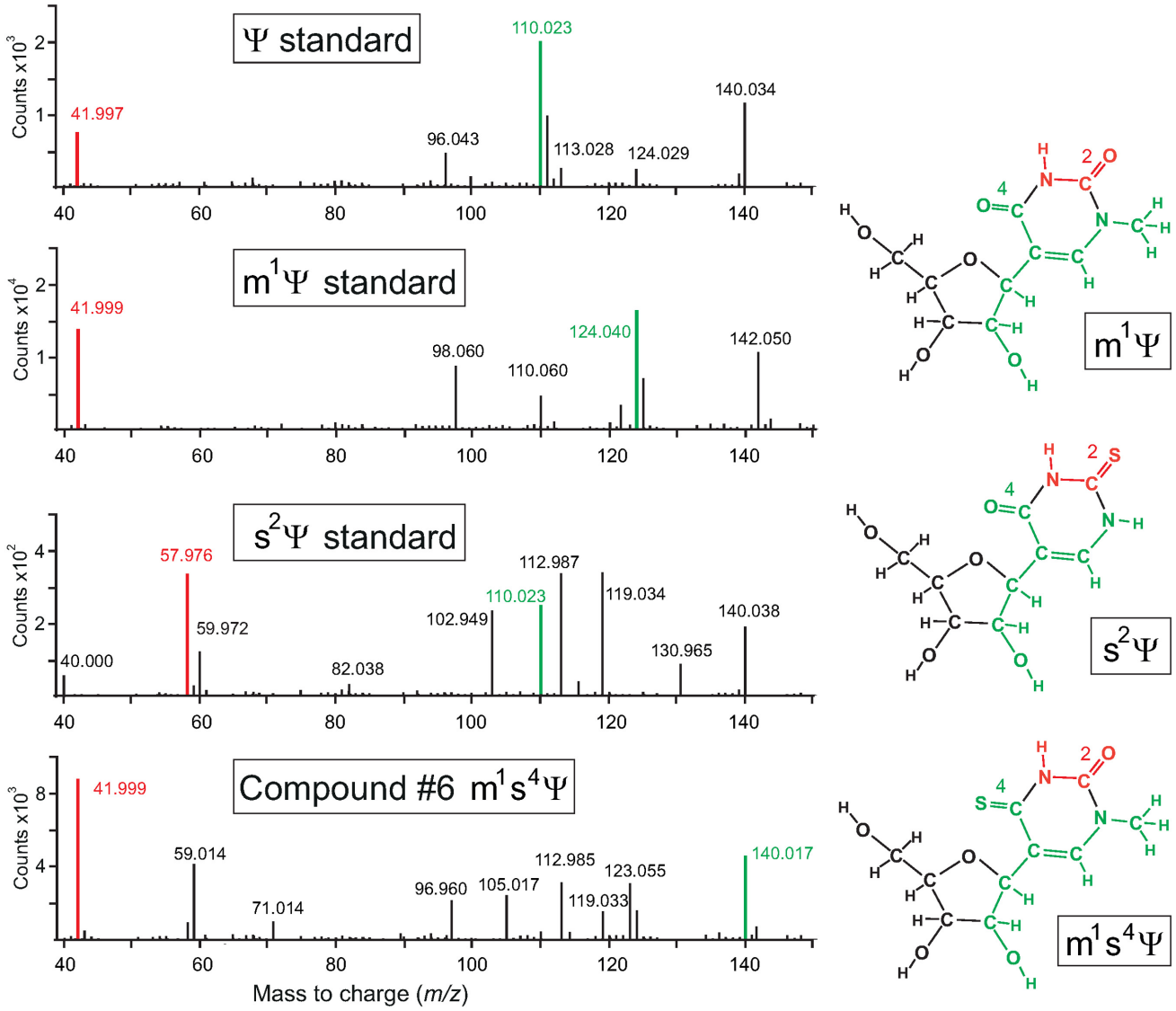

Figure 5. Tandem MS spectrum of nucleoside compound #6 in negative ion mode, comparing the measured *m/z* values of its fragmentation pattern to those of the Ψ, $m^1\Psi$ and $s^2\Psi$ standards. The fragment containing the uracil *C2* and *N3* atoms (red) has a theoretical *m/z* of 41.999 in negative ion mode when containing a *C2*-carbonyl group (the values measured here were *m/z* 41.997 for Ψ, and *m/z* 41.999 for $m^1\Psi$ and compound #6). This fragment shifts to *m/z* 57.976 when *C2* is thiolated (as for $s^2\Psi$, and not for compound #6). The fragment (in green) spanning from the *C4*-carbonyl and the *N1* atom through the glycosidic bond to the 2′-hydroxyl is seen at *m/z* 110.023 when unmodified (e.g. for Ψ and $s^2\Psi$); this fragment increases to *m/z* 124.040 when there is an *N1*-methyl group (as in $m^1\Psi$); and with a further increase to *m/z* 140.017 when the *C4*-position is thiolated (as in compound #6). With the instrumentation used here, the *m/z* measurement of 140.017 is of sufficient accuracy to distinguish the composition of this fragment as C_6H_7NOS, as opposed to the *m/z* 140.034 and 142.050 fragments, which fit the compositions $C_6H_7NO_3$ and $C_6H_9NO_3$, respectively. The data are fully consistent with compound #6 being $m^1s^4\Psi$.

performed a set of experiments to find the main methylation target of NEQ053 and to see whether any additional sites were modified.

The location of the m^5U at position 54 within the tRNA was established *in vitro* using a recombinant version of the NEQ053 enzyme with a transcript of the *N. equitans* $tRNA^{Thr}$ as its substrate (Figure 2). Under the *in vitro* conditions used, methylation by the recombinant enzyme was stoichiometric (Figure 2C). Expressing the enzyme in an *E. coli* strain where *rlmC, rlmD* and *trmA* had been inactivated (50), and thus lacked m^5U modifications in its rRNAs and tRNAs, led to m^5U modification of the tRNAs (Supplementary Figure S1). Notably, this modification was introduced into *E. coli* tRNAs *in vivo* at 37 °C, despite this growth temperature being considerably below that at which NEQ053 operates within its natural host. This is reminiscent of a 16S rRNA-specific recombinant *I. hospitalis* methyltransferase that was previously shown to function in *E. coli* cells (49).

Analysis of the nucleotide regions around 23S rRNA U747 and U1939 by MALDI-MS (53) in the *E.coli* null strain showed that there was no rescue of these modifications by the recombinant NEQ053. Analysis of the equivalent positions within *N. equitans* 23S rRNA

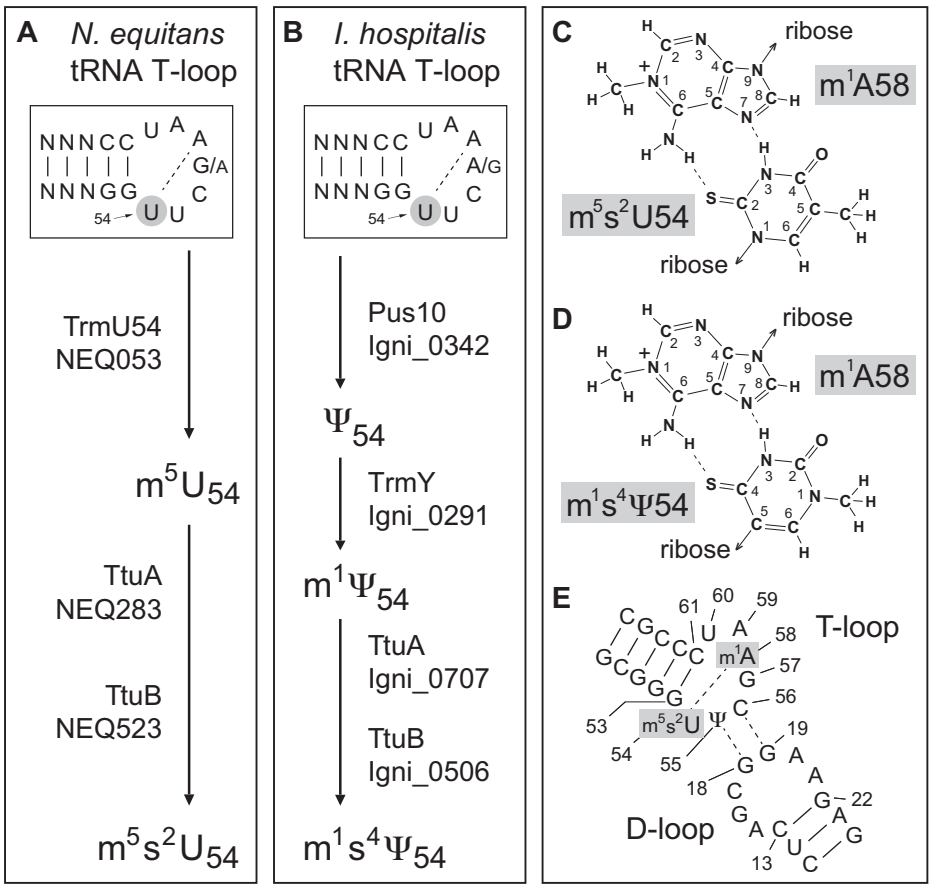

Figure 6. Modification pathways of nucleotide U54 within the tRNAs of (**A**) *N. equitans* and (**B**) *I. hospitalis*. Modified U54 makes a reverse Hoogsteen interaction with nucleotide 58 in the T-loops of both archaea where (**C**) the m^5s^2U54 to m^1A58 interaction in *N. equitans* is functionally equivalent to (**D**) the $m^1s^4\Psi54$ to m^1A58 pair found in *I. hospitalis*. (**E**) Putative interaction of the archaeal tRNA D- and T-loops based on the yeast $tRNA^{Phe}$ structure (33). The *N. equitans* and *I. hospitalis* genomes respectively encode the m^1A methyltransferase TrmI homologs Igni_1131 and NEQ337. The presence of m^1A was confirmed by LC (retention time of 3.6 min) and by ESI-MS/MS (not shown) in the tRNAs of both archaea; m^1I (LC retention time of 3.6 min) was also found in both species, and presumably is formed at position 57 via an m^1A intermediate in tRNAs that have an adenosine at this position (67,68). MS fragmentation confirmed the structures of Ψ (Figure 5), m^5s^2U54 (Figure 3) and $m^1s^4\Psi54$ (Figures 4 and 5).

similarly showed that there was no m^5U modification (Supplementary Figure S2). Taken together with the tRNA modification data, this suggests that the activity of the recombinant NEQ053 in the heterologous host reflects how the enzyme functions in *N. equitans*.

While ruling out m^5U modifications in the *N. equitans* 23S rRNA, the MS analyses in combination with primer extension unearthed numerous sites of 2′-*O*-methylation within the structures around nucleotide 1939 (Supplementary Figure S2). Extensive 2′-*O*-methylation and a paucity of nucleobase modifications has previously been noted in the 3′-minor domain of *N. equitans* 16S rRNA and could represent a means of facilitating ribosomal subunit maturation and function (49). In the present case, this would suggest that the role of m^5U1939 in 23S rRNA might also be substituted by other modifications at neighbouring nucleotides.

All these findings are consistent with the exclusive function of NEQ053 being to add the m^5U54 modification in *N. equitans* tRNAs, and this enzyme can thus be renamed as TrmU54 with the same classification as the PAB0719 enzyme (9,26). Assuming the presence of one m^5U54 per fully matured tRNA, as seen in most organisms (2,3,59,60), the proportion of m^5U in *N. equitans* tRNAs would be around 12% of the total uridine content (Figure 2C) rather than the 3% observed here. This small proportion of *N. equitans* tRNAs containing m^5U54 was subsequently shown to represent a transient stage of their maturation process, prior to hypermodification of this nucleotide position (Figure 6A). *In silico* screening revealed homologs of TtuA and TtuB that thiolate the 2-position of m^5U in the tRNAs of some thermophilic bacteria (46), where TtuA acts as a 2-thio synthetase and TtuB as a sulphur carrier/donor (61,62). The *N. equitans* ORF NEQ283 showed high similarity to PF0273 (TtuA homolog) from *P. furiosus*, while NEQ523 displayed even closer resemblance to the TtuB homolog PF1758. Genes encoding homologous enzymes are also apparent in the genomes of other Nanoarchaeota. LC/ESI-MS analyses of the *N. equitans* tRNAs unequivocally showed the presence of m^5s^2U (Figure 4). Nucleotide m^5s^2U at tRNA position 54 has been noted in other hyperthermophiles, where the relative proportions of m^5U that is thiolated to m^5s^2U varies with environmental conditions and in particular the

growth temperature (10,11,13,15). This modified nucleotide is absent in the *I. hospitalis* tRNAs (Table 1).

A search for alternative U54 modification pathways in *I. hospitalis* tRNAs revealed Igni_0342, which is a homolog of the *P. abyssi* enzyme Pus10 that isomerizes both this nucleotide and its neighbour U55 to Ψ (47). In a subsequent modification step seen in many archaeal species, Ψ54 is converted to $m^1\Psi$ by the TrmY methyltransferase (47). Bioinformatics analysis indicated that the methylation reaction is most likely carried out by Igni_0291, which resembles PAB1866, the *P. abyssi* homolog of TrmY. Not surprisingly, no homologs of Pus10 or TrmY are present in *N. equitans*. Intriguingly, however, the *I. hospitalis* genome encodes orthologs of the two putative U54 thiolation enzymes, where Igni_0707 resembles NEQ283, and Igni_0506 is similar to NEQ523, raising the possibility that *I. hospitalis* might thiolate $m^1\Psi$54. LC fractionation and ESI-MS analyses confirmed that this is indeed the case, and *I. hospitalis* tRNAs contain the previously uncharacterized nucleoside $m^1s^4\Psi$ (Figures 4 and 5). The enzymatic steps involved in $m^1s^4\Psi$ synthesis are summarized in Figure 6B, and homologs of these enzymes are evident in other Crenarchaeota including the close relative, *Ignicoccus islandicus*.

Modification of U54 helps maintain the highly conserved L-shaped tertiary structure of tRNAs, facilitating interaction with elongation factors and ribosomal binding sites during the course of mRNA translation (63,64). Here, the reverse Hoogsteen interaction between nucleotides 54 and 58 plays a key role in maintaining the internal structure of the T-loop and its contacts with the D-loop (33). Nucleotide 54, hypermodified as m^5s^2U in *N. equitans* and $m^1s^4\Psi$ in *I. hospitalis* would be conformed in an essentially identical manner with the 2-thiol group in m^5s^2U (Figure 6C) and 4-thio group of $m^1s^4\Psi$ (Figure 6D) in the same relative position holding the ribose of nucleotide-54 in a C3′-*endo*-pucker and the glycosidic bond in the *anti*-configuration to avoid steric clash with the 2′-hydroxyl. This, in conjunction with the 5-methyl of m^5s^2U and the equivalently-positioned 1-methyl of $m^1s^4\Psi$, would strengthen nucleotide-54 stacking between nucleotides 53 and 55.

Uridine 55 is isomerized to pseudouridine in most tRNAs, and Ψ is present in both *N. equitans* and *I. hospitalis* tRNAs (Table 1). The stacked arrangement optimally positions both m^5s^2U54 and $m^1s^4\Psi$54 to make the reverse Hoogsteen pairing with A58, which is itself stacked between G57 and C61. Extrapolating from the yeast $tRNA^{Phe}$ crystal structure, this arrangement facilitates the interaction of Ψ55 and C56 with the D-loop nucleotides 19 and 18 (Figure 6E), respectively, and enables nucleotides 59 and 60 to coordinate a magnesium ion with the D-loop (33). The identities of yeast $tRNA^{Phe}$ nucleotides 59 and 60 are different than in the archaeal tRNAs (Figure 2) where the D-loops lack dihydrouridine (65), and while metal ion coordination between these archaeal positions remains structurally feasible, it remains to be demonstrated. The T-loop structure is further strengthened by m^1A58 modification in species of Archaea, Bacteria and Eukarya (66). Nucleoside m^1A was identified in both the *I. hospitalis* and *N. equitans* tRNAs (Figure 6E legend).

Further screening of the archaeal tRNAs revealed a total of eleven modified forms of uridine (Table 1). Both archaea contained unmodified uridine, Ψ, Um, s^2U and s^4U in their tRNAs, while nucleotides m^5U, m^5s^2U and a thiolated pseudouridine (compound #9) are specific to *N. equitans,* and $m^1\Psi$, $m^1s^4\Psi$, $m^1\Psi m$ and s^2Um are specific to *I. hospitalis*. In a study of tRNA modifications in fourteen diverse archaeal species, s^2Um was confined to the hyperthermophilic Crenarchaeota branch of the Archaea and absent from both the Euryarchaeota and Bacteria (10). Our findings are consistent with this previous study, and we note that although *N. equitans* lacks s^2Um in its tRNAs, it does produce both Um and s^2U.

In conclusion, we demonstrate here that while *N. equitans* and *I. hospitalis* grow physically attached under identical hyperthermic conditions, their modifications at U54 in their tRNAs are determined by their phylogenetic origins. These two organisms thus possess structural solutions that have evolved independently and convergently to ensure tRNA function within this extreme environment.

SUPPLEMENTARY DATA

Supplementary Data are available at NAR Online.

ACKNOWLEDGEMENTS

We thank Basma El Yacoubi and Valérie de Crécy-Lagard, University of Florida in Gainsville for advice on cloning of NEQ053, Kenneth Holst Seistrup for help with bioinformatics analyses. The Villum Center for Bioanalytical Sciences is thanked for providing access to mass spectrometric equipment.

FUNDING

Danish Research Agency [FNU rammebevilling 10-084554 to S.D.]; Deutsche Forschungsgemeinschaft [Förderkennzeichen HU701/2 to H.H.]. Funding for open access charge: FNU-rammebevilling [10-084554 to S.D.].
Conflict of interest statement. None declared.

REFERENCES

1. Ofengand,J. and Del Campo,M. (2005) Modified nucleotides of *E. coli* ribosomal RNA. In: Böck,A., Curtis,R., Kaper,J.B., Neidhardt,T., Nyström,T. and Squires,C. (eds). *Escherichia coli and Salmonella*. ASM Press, Washington, DC.
2. Björk,G.R. and Hagervall,T.G. (2005) In: Böck,A., Curtis,R., Kaper,J.B., Neidhardt,T., Nyström,T. and Squires,C. (eds). *Escherichia coli and Salmonella*. ASM Press, Washington DC.
3. Grosjean,H. (2009) Nucleic Acids are not boring long polymers of only four types of nucleotides. In: Grosjean,H. (ed). DNA and RNA modification enzymes: Structure, mechanism, function and evolution. Landes Biosciences, Austin, Texas. pp. 1–18.
4. Agris,P.F., Narendran,A., Sarachan,K., Vare,V.Y.P. and Eruysal,E. (2017) The Importance of Being Modified: The Role of RNA Modifications in Translational Fidelity. *Enzymes*, **41**, 1–50.
5. Boccaletto,P., Machnicka,M.A., Purta,E., Piatkowski,P., Baginski,B., Wirecki,T.K., de Crecy-Lagard,V., Ross,R., Limbach,P.A., Kotter,A. *et al.* (2018) MODOMICS: a database of RNA modification pathways. 2017 update. *Nucleic Acids Res.*, **46**, D303–D307.
6. Hsuchen,C.C. and Dubin,D.T. (1980) Methylation patterns of mycoplasma transfer and ribosomal ribonucleic acid. *J. Bacteriol.*, **144**, 991–998.

7. Johnson,L., Hayashi,H. and Söll,D. (1970) Isolation and properties of a transfer ribonucleic acid deficient in ribothymidine. *Biochemistry*, **9**, 2823–2831.
8. Grosjean,H., Breton,M., Sirand-Pugnet,P., Tardy,F., Thiaucourt,F., Citti,C., Barre,A., Yoshizawa,S., Fourmy,D., de Crecy-Lagard,V. *et al.* (2014) Predicting the minimal translation apparatus: lessons from the reductive evolution of mollicutes. *PLoS Genet.*, **10**, e1004363.
9. Urbonavičius,J., Auxilien,S., Walbott,H., Trachana,K., Golinelli-Pimpaneau,B., Brochier-Armanet,C. and Grosjean,H. (2008) Acquisition of a bacterial RumA-type tRNA(uracil-54, C5)-methyltransferase by Archaea through an ancient horizontal gene transfer. *Mol. Microbiol.*, **67**, 323–335.
10. Edmonds,C.G., Crain,P.F., Gupta,R., Hashizume,T., Hocart,C.H., Kowalak,J.A., Pomerantz,S.C., Stetter,K.O. and McCloskey,J.A. (1991) Posttranscriptional modification of tRNA in thermophilic archaea (Archaebacteria). *J. Bacteriol.*, **173**, 3138–3148.
11. Kowalak,J.A., Dalluge,J.J., McCloskey,J.A. and Stetter,K.O. (1994) The role of posttranscriptional modification in stabilization of transfer RNA from hyperthermophiles. *Biochemistry*, **33**, 7869–7876.
12. Watanabe,K., Oshima,T., Saneyoshi,M. and Nishimura,S. (1974) Replacement of ribothymidine by 5-methyl-2-thiouridine in sequence GTΨC in tRNA of an extreme thermophile. *FEBS Lett.*, **43**, 59–63.
13. Watanabe,K., Oshima,T., Hansske,F. and Ohta,T. (1983) Separation and comparison of 2-thioribothymidine-containing transfer ribonucleic acid and the ribothymidine-containing counterpart from cells of *Thermus thermophilus* HB 8. *Biochemistry*, **22**, 98–102.
14. Shigi,N., Suzuki,T., Tamakoshi,M., Oshima,T. and Watanabe,K. (2002) Conserved bases in the TΨC loop of tRNA are determinants for thermophile-specific 2-thiouridylation at position 54. *J. Biol. Chem.*, **277**, 39128–39135.
15. Shigi,N., Suzuki,T., Terada,T., Shirouzu,M., Yokoyama,S. and Watanabe,K. (2006) Temperature-dependent biosynthesis of 2-thioribothymidine of *Thermus thermophilus* tRNA. *J. Biol. Chem.*, **281**, 2104–2113.
16. Grosjean,H. and Oshima,T. (2007) How Nucleic Acids cope with high temperature. In: Gerday,C. and Glansdorff,N. (eds). *Physiology and Biochemistry of Extremophiles*. ASM Press, pp. 39–56.
17. Lorenz,C., Lunse,C.E. and Morl,M. (2017) tRNA modifications: impact on structure and thermal adaptation. *Biomolecules*, **7**, 35.
18. Phillips,G. and de Crecy-Lagard,V. (2011) Biosynthesis and function of tRNA modifications in Archaea. *Curr. Opin. Microbiol.*, **14**, 335–341.
19. Hori,H., Kawamura,T., Awai,T., Ochi,A., Yamagami,R., Tomikawa,C. and Hirata,A. (2018) Transfer RNA modification enzymes from thermophiles and their modified nucleosides in tRNA. *Microorganisms*, **6**, 110.
20. Tatusov,R.L., Fedorova,N.D., Jackson,J.D., Jacobs,A.R., Kiryutin,B., Koonin,E.V., Krylov,D.M., Mazumder,R., Mekhedov,S.L., Nikolskaya,A.N. *et al.* (2003) The COG database: an updated version includes eukaryotes. *BMC Bioinformatics*, **4**, 41.
21. Anantharaman,V., Koonin,E.V. and Aravind,L. (2002) Comparative genomics and evolution of proteins involved in RNA metabolism. *Nucleic Acids Res.*, **30**, 1427–1464.
22. Ny,T., Lindstrom,H.R., Hagervall,T.G. and Björk,G.R. (1988) Purification of transfer RNA m^5U54-methyltransferase from *Escherichia coli*. Association with RNA. *Eur. J. Biochem.*, **177**, 467–475.
23. Gu,X., Ivanetich,K.M. and Santi,D.V. (1996) Recognition of the T-arm of tRNA by tRNA m^5U54 -methyltransferase is not sequence specific. *Biochemistry*, **35**, 11652–11659.
24. Alian,A., Lee,T.T., Griner,S.L., Stroud,R.M. and Finer-Moore,J. (2008) Structure of a TrmA-RNA complex: A consensus RNA fold contributes to substrate selectivity and catalysis in m^5U methyltransferases. *Proc. Natl Acad. Sci. U.S.A.*, **105**, 6876–6881.
25. Nordlund,M.E., Johansson,J.O., von Pawel-Rammingen,U. and Byström,A.S. (2000) Identification of the TRM2 gene encoding the tRNA (m^5U54) methyltransferase of *Saccharomyces cerevisiae*. *RNA*, **6**, 844–860.
26. Walbott,H., Leulliot,N., Grosjean,H. and Golinelli-Pimpaneau,B. (2008) The crystal structure of *Pyrococcus abyssi* tRNA (uracil-54, C5)-methyltransferase provides insights into its tRNA specificity. *Nucleic. Acids. Res.*, **36**, 4929–4940.
27. Delk,A.S. and Rabinowitz,J.C. (1975) Biosynthesis of ribosylthymine in the transfer RNA of *Streptococcus faecalis*: a folate-dependent methylation not involving S-adenosylmethionine. *Proc. Natl. Acad. Sci. U.S.A.*, **72**, 528–530.
28. Urbonavičius,J., Brochier-Armanet,C., Skouloubris,S., Myllykallio,H. and Grosjean,H. (2007) In vitro detection of the enzyme activity of folate-dependent tRNA(U54, C5)-methyltransferase. *Methods Enzymol.*, **425**, 103–119.
29. Urbonavičius,J., Skouloubris,S., Myllykallio,H. and Grosjean,H. (2005) Identification of a novel gene encoding a flavin-dependent tRNA:m^5U methyltransferase in bacteria-evolutionary implications. *Nucleic. Acids Res.*, **33**, 3955–3964.
30. Yamagami,R., Yamashita,K., Nishimasu,H., Tomikawa,C., Ochi,A., Iwashita,C., Hirata,A., Ishitani,R., Nureki,O. and Hori,H. (2012) The tRNA recognition mechanism of folate/FAD-dependent tRNA methyltransferase (TrmFO). *J. Biol. Chem.*, **287**, 42480–42494.
31. Hamdane,D., Argentini,M., Cornu,D., Golinelli-Pimpaneau,B. and Fontecave,M. (2012) FAD/folate-dependent tRNA methyltransferase: flavin as a new methyl-transfer agent. *J. Am. Chem. Soc.*, **134**, 19739–19745.
32. Watanabe,K., Yokoyama,S., Hansske,F., Kasai,H. and Miyazawa,T. (1979) CD and NMR studies on the conformational thermostability of 2-thioribothymidine found in the TΨC loop of thermophile tRNA. *Biochem. Biophys. Res. Commun.*, **91**, 671–677.
33. Shi,H. and Moore,P.B. (2000) The crystal structure of yeast phenylalanine tRNA at 1.93 A resolution: a classic structure revisited. *RNA*, **6**, 1091–1105.
34. Horie,N., Hara-Yokoyama,M., Yokoyama,S., Watanabe,K., Kuchino,Y., Nishimura,S. and Miyazawa,T. (1985) Two $tRNA^{Ile1}$ species from an extreme thermophile, *Thermus thermophilus* HB8: effect of 2-thiolation of ribothymidine on the thermostability of tRNA. *Biochemistry*, **24**, 5711–5715.
35. Davanloo,P., Sprinzl,M., Watanabe,K., Albani,M. and Kersten,H. (1979) Role of ribothymidine in the thermal stability of transfer RNA as monitored by proton magnetic resonance. *Nucleic Acids Res.*, **6**, 1571–1581.
36. Pang,H., Ihara,M., Kuchino,Y., Nishimura,S., Gupta,R., Woese,C.R. and McCloskey,J.A. (1982) Structure of a modified nucleoside in archaebacterial tRNA which replaces ribosylthymine. 1-Methylpseudouridine. *J. Biol. Chem.*, **257**, 3589–3592.
37. Romby,P., Carbon,P., Westhof,E., Ehresmann,C., Ebel,J.P., Ehresmann,B. and Giege,R. (1987) Importance of conserved residues for the conformation of the T-loop in tRNAs. *J. Biomol. Struct. Dyn.*, **5**, 669–687.
38. Jahn,U., Gallenberger,M., Paper,W., Junglas,B., Eisenreich,W., Stetter,K.O., Rachel,R. and Huber,H. (2008) *Nanoarchaeum equitans* and *Ignicoccus hospitalis*: new insights into a unique, intimate association of two archaea. *J. Bacteriol.*, **190**, 1743–1750.
39. Huber,H., Hohn,M.J., Rachel,R., Fuchs,T., Wimmer,V.C. and Stetter,K.O. (2002) A new phylum of Archaea represented by a nanosized hyperthermophilic symbiont. *Nature*, **417**, 63–67.
40. Forterre,P., Gribaldo,S. and Brochier-Armanet,C. (2009) Happy together: genomic insights into the unique *Nanoarchaeum/Ignicoccus* association. *J. Biol.*, **8**, 7.
41. Rinke,C., Schwientek,P., Sczyrba,A., Ivanova,N.N., Anderson,I.J., Cheng,J.F., Darling,A., Malfatti,S., Swan,B.K., Gies,E.A. *et al.* (2013) Insights into the phylogeny and coding potential of microbial dark matter. *Nature*, **499**, 431–437.
42. Podar,M., Anderson,I., Makarova,K.S., Elkins,J.G., Ivanova,N., Wall,M.A., Lykidis,A., Mavromatis,K., Sun,H., Hudson,M.E. *et al.* (2008) A genomic analysis of the archaeal system *Ignicoccus hospitalis-Nanoarchaeum equitans*. *Genome Biol.*, **9**, R158.
43. Waters,E., Hohn,M.J., Ahel,I., Graham,D.E., Adams,M.D., Barnstead,M., Beeson,K.Y., Bibbs,L., Bolanos,R., Keller,M. *et al.* (2003) The genome of *Nanoarchaeum equitans*: insights into early archaeal evolution and derived parasitism. *Proc. Natl. Acad. Sci. U.S.A.*, **100**, 12984–12988.
44. Altschul,S.F., Gish,W., Miller,W., Myers,E.W. and Lipman,D.J. (1990) Basic local alignment search tool. *J. Mol. Biol.*, **215**, 403–410.
45. Lartigue,C., Lebaudy,A., Blanchard,A., Yacoubi,B.E., Rose,S., Grosjean,H. and Douthwaite,S. (2014) The flavoprotein Mcap0476 (RlmFO) catalyzes m^5U1939 modification in *Mycoplasma capricolum* 23S rRNA. *Nucleic Acids Res.*, **42**, 8073–8082.

46. Shigi,N., Sakaguchi,Y., Suzuki,T. and Watanabe,K. (2006) Identification of two tRNA thiolation genes required for cell growth at extremely high temperatures. *J. Biol. Chem.*, **281**, 14296–14306.
47. Chatterjee,K., Blaby,I.K., Thiaville,P.C., Majumder,M., Grosjean,H., Yuan,Y.A., Gupta,R. and de Crecy-Lagard,V. (2012) The archaeal COG1901/DUF358 SPOUT-methyltransferase members, together with pseudouridine synthase Pus10, catalyze the formation of 1-methylpseudouridine at position 54 of tRNA. *RNA*, **18**, 421–433.
48. Giessing,A.M., Jensen,S.S., Rasmussen,A., Hansen,L.H., Gondela,A., Long,K., Vester,B. and Kirpekar,F. (2009) Identification of 8-methyladenosine as the modification catalyzed by the radical SAM methyltransferase Cfr that confers antibiotic resistance in bacteria. *RNA*, **15**, 327–336.
49. Seistrup,K.H., Rose,S., Birkedal,U., Nielsen,H., Huber,H. and Douthwaite,S. (2017) Bypassing rRNA methylation by RsmA/Dim1 during ribosome maturation in the hyperthermophilic archaeon *Nanoarchaeum equitans*. *Nucleic Acids Res.*, **45**, 2007–2015.
50. Desmolaize,B., Fabret,C., Bregeon,D., Rose,S., Grosjean,H. and Douthwaite,S. (2011) A single methyltransferase YefA (RlmCD) catalyses both m^5U747 and m^5U1939 modifications in *Bacillus subtilis* 23S rRNA. *Nucleic Acids Res.*, **39**, 9368–9375.
51. Auxilien,S., Rasmussen,A., Rose,S., Brochier-Armanet,C., Husson,C., Fourmy,D., Grosjean,H. and Douthwaite,S. (2011) Specificity shifts in the rRNA and tRNA nucleotide targets of archaeal and bacterial m^5U methyltransferases. *RNA*, **17**, 45–53.
52. Grosjean,H., Droogmans,L., Roovers,M. and Keith,G. (2007) Detection of enzymatic activity of transfer RNA modification enzymes using radiolabelled tRNA substrates. *Methods Enzymol.*, **425**, 57–101.
53. Madsen,C.T., Mengel-Jorgensen,J., Kirpekar,F. and Douthwaite,S. (2003) Identifying the methyltransferases for m^5U747 and m^5U1939 in 23S rRNA using MALDI mass spectrometry. *Nucleic Acids Res.*, **31**, 4738–4746.
54. Andersen,T.E., Porse,B.T. and Kirpekar,F. (2004) A novel partial modification at 2501 in *Escherichia coli* 23S ribosomal RNA. *RNA*, **10**, 907–913.
55. Douthwaite,S. and Kirpekar,F. (2007) Identifying modifications in RNA by MALDI mass spectrometry. *Methods Enzymol.*, **425**, 3–20.
56. Stern,S., Moazed,D. and Noller,H.F. (1988) Structural analysis of RNA using chemical and enzymatic probing monitored by primer extension. *Methods Enzymol.*, **164**, 481–489.
57. Agarwalla,S., Kealey,J.T., Santi,D.V. and Stroud,R.M. (2002) Characterization of the 23S ribosomal RNA m^5U1939 methyltransferase from *Escherichia coli*. *J. Biol. Chem.*, **277**, 8835–8840.
58. Purta,E., O'Connor,M., Bujnicki,J.M. and Douthwaite,S. (2008) YccW is the m^5C methyltransferase specific for 23S rRNA nucleotide 1962. *J. Mol. Biol.*, **383**, 641–651.
59. Jühling,F., Mörl,M., Hartmann,R.K., Sprinzl,M., Stadler,P.F. and Pütz,J. (2009) tRNAdb 2009: compilation of tRNA sequences and tRNA genes. *Nucleic. Acids. Res.*, **37**, D159–162.
60. Barraud,P. and Tisné,C. (2019) To be or not to be modified: Miscellaneous aspects influencing nucleotide modifications in tRNAs. *IUBMB Life*, **71**, 1126–1140.
61. Arragain,S., Bimai,O., Legrand,P., Caillat,S., Ravanat,J.L., Touati,N., Binet,L., Atta,M., Fontecave,M. and Golinelli-Pimpaneau,B. (2017) Nonredox thiolation in tRNA occurring via sulfur activation by a [4Fe-4S] cluster. *Proc. Natl. Acad. Sci. U.S.A.*, **114**, 7355–7360.
62. Chen,M., Asai,S.I., Narai,S., Nambu,S., Omura,N., Sakaguchi,Y., Suzuki,T., Ikeda-Saito,M., Watanabe,K., Yao,M. *et al.* (2017) Biochemical and structural characterization of oxygen-sensitive 2-thiouridine synthesis catalyzed by an iron-sulfur protein TtuA. *Proc. Natl. Acad. Sci. U.S.A.*, **114**, 4954–4959.
63. Selmer,M., Dunham,C.M., Murphy,F.V.t., Weixlbaumer,A., Petry,S., Kelley,A.C., Weir,J.R. and Ramakrishnan,V. (2006) Structure of the 70S ribosome complexed with mRNA and tRNA. *Science*, **313**, 1935–1942.
64. Zhang,J. and Ferre-D'Amare,A.R. (2016) The tRNA Elbow in Structure, Recognition and Evolution. *Life (Basel)*, **6**, 3.
65. Noon,K.R., Guymon,R., Crain,P.F., McCloskey,J.A., Thomm,M., Lim,J. and Cavicchioli,R. (2003) Influence of temperature on tRNA modification in archaea: *Methanococcoides burtonii* (optimum growth temperature [T_{opt}], 23 degrees C) and *Stetteria hydrogenophila* (T_{opt} 95 degrees C). *J. Bacteriol.*, **185**, 5483–5490.
66. Guelorget,A., Roovers,M., Guerineau,V., Barbey,C., Li,X. and Golinelli-Pimpaneau,B. (2010) Insights into the hyperthermostability and unusual region-specificity of archaeal *Pyrococcus abyssi* tRNA $m^1A57/58$ methyltransferase. *Nucleic Acids Res.*, **38**, 6206–6218.
67. Grosjean,H., Constantinesco,F., Foiret,D. and Benachenhou,N. (1995) A novel enzymatic pathway leading to 1-methylinosine modification in *Haloferax volcanii* tRNA. *Nucleic Acids Res.*, **23**, 4312–4319.
68. Roovers,M., Wouters,J., Bujnicki,J.M., Tricot,C., Stalon,V., Grosjean,H. and Droogmans,L. (2004) A primordial RNA modification enzyme: the case of tRNA (m^1A) methyltransferase. *Nucleic Acids Res.*, **32**, 465–476.